NANO LETTERS

2002
Vol. 2, No. 12
1413−1417

Covalently Bonded Adducts of Deoxyribonucleic Acid (DNA) Oligonucleotides with Single-Wall Carbon Nanotubes: Synthesis and Hybridization

Sarah E. Baker, Wei Cai, Tami L. Lasseter, Kevin P. Weidkamp, and Robert J. Hamers*

Department of Chemistry, University of Wisconsin-Madison, 1101 University Avenue, Madison, Wisconsin 53706

Received August 1, 2002; Revised Manuscript Received September 13, 2002

ABSTRACT

We have developed a multistep route to the formation of covalently linked adducts of single-wall carbon nanotubes (SWNT) and deoxyribonucleic acid (DNA) oligonucleotides. X-ray photoelectron spectroscopy was used to characterize the initial chemical modification to form amine-terminated SWNTs, which were then covalently linked to DNA. The resulting DNA–SWNT adducts hybridize selectively with complementary sequences, with only minimal interaction with noncomplementary sequences.

Many of the most interesting and unique properties of nanoscale materials are realized only when they are integrated into more complex assemblies.[1,2] In biology, the highly selective binding between complementary sequences of deoxyribonucleic acid (DNA) plays the central role in genetic replication. This selectivity can, in principle, be used to assemble a wider range of materials, by forming adducts between DNA and the material of interest.[3] While biomolecules such as DNA can be linked to nanotubes via noncovalent interactions,[4−7] the use of covalent chemistry is expected to provide the best stability, accessibility, and selectivity during competitive hybridization. Here, we report a multistep route for covalently linking DNA to single-wall carbon nanotubes (SWNTs). We find that DNA molecules covalently linked to SWNTs are accessible to hybridization and strongly favor hybridization with molecules having complementary sequences compared with noncomplementary sequences.

Figure 1 shows an overview of the covalent attachment process. Purified SWNTs were oxidized to form carboxylic acid groups at the ends and sidewalls (Figure 1b). These were reacted with thionyl chloride and then ethylenediamine to produce amine-terminated sites (Figure 1c). The amines were then reacted with the heterobifunctional cross-linker succinimidyl 4-(*N*-maleimidomethyl)cyclohexane-1-carboxylate, (SMCC), leaving the surface terminated with maleimide groups (Figure 1d). Finally, thiol-terminated DNA was reacted with these groups to produce DNA-modified SWNTs (Figure 1e).

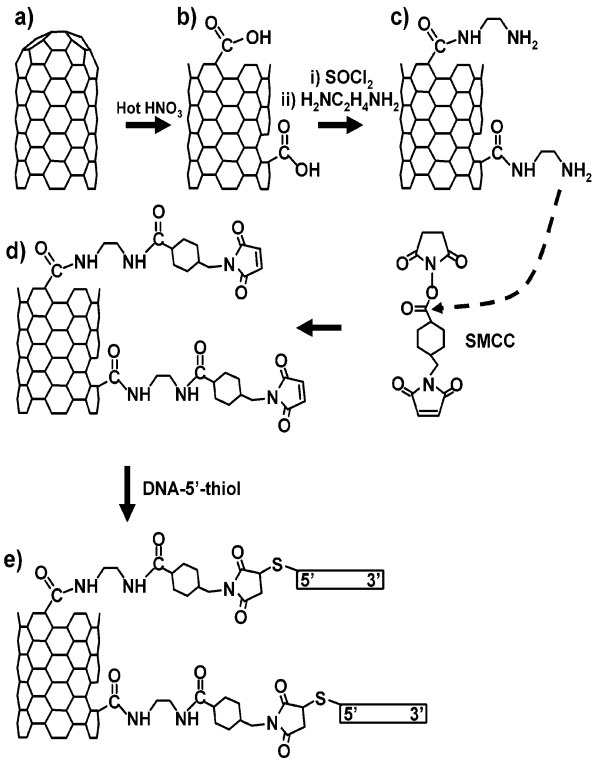

Figure 1. Overall scheme for fabrication of covalently linked DNA−nanotube adducts.

* Corresponding author. E-mail: rjhamers@facstaff.wisc.edu

10.1021/nl025729f CCC: $22.00
Published on Web 10/05/2002

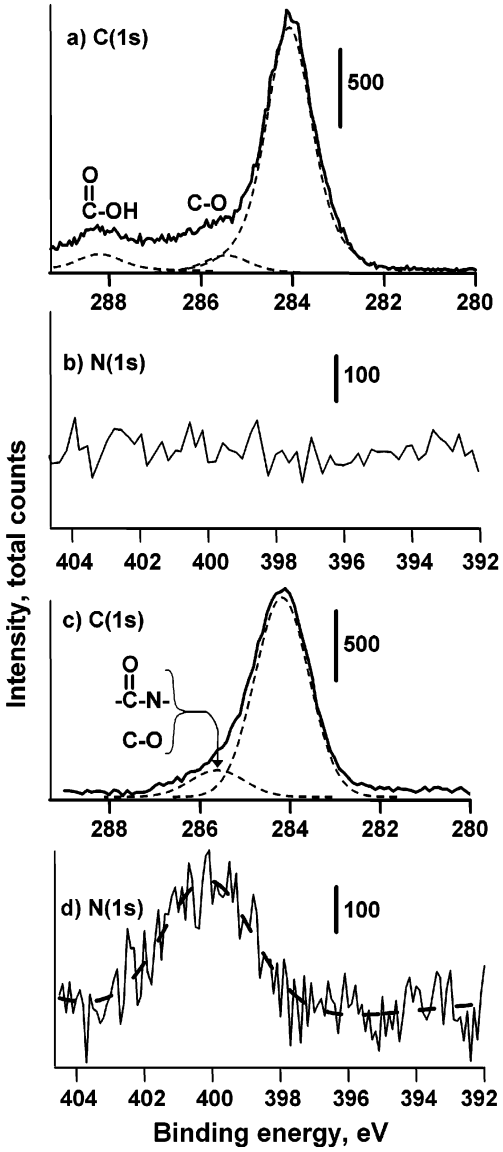

Figure 2. X-ray photoelectron spectroscopy of chemically modified nanotubes. (a) C(1s) spectrum of oxidized nanotubes, along with fit to three peaks as described in text. (b) N(1s) spectrum of oxidized nanotubes, showing no detectable N(1s) signal. (c) C(1s) spectrum of oxidized nanotubes functionalized after reaction with $SOCl_2$ and then ethylenediamine, showing elimination of the acid carbonyl peak near 288 eV and increased intensity near 286−286.5 eV from the amide group. (d) N(1s) spectrum of oxidized nanotubes functionalized with ethylenediamine.

Single-wall nanotubes (Carbolex, Lexington, Ky) were first purified[8,9] by refluxing the as-received nanotubes in 3 M nitric acid for 24 h and then washing the SWNTs with water using a 0.6 micron polycarbonate membrane filter (Millipore). Elemental analysis (Desert Analytics) showed that this procedure reduces the Ni contamination from 19% to 4.0 wt %, and the Yttrium contamination from 4.8% to 0.75%. Previous studies have shown that this procedure results in partial oxidation of the nanotubes, leaving carboxylic acid groups at the nanotube ends and at sidewall defect sites.[10] Figure 2 shows a C(1s) X-ray photoelectron spectrum of the oxidized nanotubes obtained under ultrahigh vacuum (UHV) conditions using a Al Kα source. The spectrum shows a large peak at 284.2 eV from the nanotubes with 88% of the total C(1s) area, a smaller shoulder at 285.9 eV (6.4% of total area), and a well-separated peak at 288.2 eV (5.9% of total area). The peak at 288.2 eV is attributed to the carbonyl groups of carboxylic acid groups, and the 4 eV difference between this peak and the main carbon peak is very close to previously reported values.[11−13] The smaller peak at 285.9 eV, 1.7 eV higher than the main carbon peak, is attributed to C atoms in ether-like linkages[13] and also to satellite peaks arising from excitation of electronic transitions within the nanotubes.[14] These results suggest that 6% of the carbon atoms are present as carbonyl groups, comparable to values previously reported using similar procedures.[15,16] The corresponding N(1s) spectrum (Figure 2b) shows no signal above the detection limit of the instrument, even with extensive signal averaging.

To functionalize the nanotubes with amine groups, the purified, oxidized material (∼60% of initial weight of SWNTs) was dried under vacuum and then suspended in 1 mL of anhydrous dimethylformamide (DMF) in an ultrasonic bath. This dispersion was immediately added to 20 mL thionyl chloride (Aldrich) and heated under reflux for 24 h to convert the carboxylic acids to acyl chlorides.[17] These nanotubes were rinsed over a 0.2 micron PTFE membrane (Millipore) with anhydrous THF to remove excess $SOCl_2$, and were then added to ethylenediamine (neat, Aldrich) and stirred for 3−5 days in order to form the product depicted in Figure 1c.

Because formation of the amine-terminated nanotubes is a critical step in the overall chemical scheme, several measurements were performed to help confirm the presence of a covalent linkage between the carbon nanotubes and ethylenediamine to form the product depicted in Figure 1c. The modified tubes were characterized by XPS after briefly warming to ∼75 °C in UHV to remove any residual physically adsorbed amines. Using the bulk C(1s) peak as an internal standard at 284.2 eV (as in Figure 2a), the resulting C(1s) photoelectron spectrum (Figure 2c) shows some broadening of the bulk peak and a shoulder near 285.5 eV, about 1.3 eV higher than the main C(1s) peak. However, there is no significant intensity near 288 eV. The absence of intensity at 288 eV is significant because the C(1s) binding energy of carbonyl groups is expected to decrease significantly when a carboxylic acid is converted to an amide, due to electron donation from the adjacent N atom. Carbon atoms in carboxylic acid groups and in amide groups typically have C(1s) binding energies ∼4.0 eV and ∼2.0 eV higher, respectively, than C atoms in alkanes.[18] Thus, the changes we observe in the C(1s) spectrum support the formation of an amide linkage on the nanotubes. The N(1s) spectrum (Figure 2d) shows a peak with a binding energy of 400.2 eV and a breadth of 3.4 eV full-width at half-maximum (fwhm). Previous studies have shown that amides and amines both have binding energies in the range of ∼399.5−400.5 eV.[18−20] Because the chemical scheme we use is expected to produce amine- and amide nitrogens in equal quantities (Figure 1c), both the energy and the comparatively large line

width are consistent with the successful formation of the product depicted in Figure 1c.

Although the N(1s) data provide only limited information about the bonding, measurement of the area of N(1s) and C(1s) peaks provides a quantitative measure of the extent of functionalization. Measurement of the peak areas yield an N(1s)/C(1s) peak area ratio of 0.058. Using atomic sensitivity factors[20] of 0.296 for C(1s)and 0.477 for N(1s), this yields a nitrogen-to-carbon ratio of 0.093. Since each ethylenediamine molecule contains two N atoms, this ratio indicates that ~5% of the nanotube sites are linked to ethylenediamine molecules. This 5% overall conversion to free amines is only slightly less than the ~6% of sites estimated to have been oxidized in the first step and is within the combined experimental error of the measurements. This, in turn, indicates that the conversion of carbonyl groups to amine groups via the procedure in Figure 1 is quite efficient.

Confirmation of covalent bonding of ethylenediamine to the SWNTs is complicated by the presence of two amine groups per ethylenediamine molecule, making it difficult to distinguish between the starting material and the final product. Consequently, further confirmation of covalent bond formation and overall efficacy of the functionalization was obtained using ^{1}H NMR spectroscopy on SWNTs reacted with dodecylamine by an identical procedure (spectrum shown in Supporting Information). A comparison of the spectrum of dodecylamine with the spectrum of nanotubes reacted with dodecylamine (both in $CDCl_3$) showed that while dodecylamine has a singlet centered at 1.17 ppm from the amine protons, this peak was not present in spectrum of the SWNT-dodecylamine reaction product. Instead, the reaction product showed a new peak with a chemical shift of 8.02 ppm, a value that is characteristic of amide protons.[21] Also, the SWNT−dodecylamine spectrum features significant broadening of the peaks in the region between 0.81 and 2.92 ppm, attributed to the aliphatic protons. Peak broadening in molecules attached to nanotubes can be attributed to the fact that molecules are forced to tumble slowly relative to the solvent molecules, and thus are not able to achieve full isotropic averaging.[22] These results further indicate that the procedure leads to covalent linkage between the acylated nanotube through an amide bond as depicted in Figure 1d. These amide bonds are located both at the walls and at the ends of the tubes, but the ratio of these type types of sites depends on the length-to-diameter ratio of the nanotubes. Scanning electron microscopy (SEM) micrographs using a Leo Gemini 1530 SEM showed almost entirely continuous nanotubes on a 500 nm field of view. Consequently, we conclude that the chemical functionalization occurs primarily at the sidewalls and that functionalization at the ends represents only a small contribution.

The final steps of DNA attachment are similar to those used previously to link DNA to surfaces of diamond[23,24] and silicon.[11] After the SWNTs were terminated with primary amine groups, they were added to a 60 mM solution of the heterobifunctional linker SMCC (Pierce) with a catalytic amount of triethylamine (Aldrich) in anhydrous DMF and stirred for 2 h in the dark. The nanotubes were then washed, resuspended in 0.1 M triethanolamine buffer (pH 7), and dried under vacuum, producing maleimide-terminated nanotubes (Figure 1d) that are reactive toward thiol-terminated DNA oligonucleotides. DNA oligonucleotides (University of Wisconsin Biotechnology Center) were deprotected and purified by reverse-phase high-performance liquid chromatography immediately before use. To form the final DNA-SWNT link, the maleimide-terminated nanotubes were immersed in 100 μM purified DNA oligonucleotide solution in triethanolamine buffer.

Several different DNA oligonucleotides were used in these experiments. To optimize the DNA−SWNT linkage, a 32-base fluorescently labeled oligonucleotide (5′-HS−C_6H_{12}-T_{15}GC TTA ACG AGC AAT CGT FAM-3′) ("S1") was used. This oligonucleotide was modified at the 5′ end using the reagent 5′-thiol modifier C6 (Glen Research) to give a thiol group for attachment to the maleimide group on the nanotubes (Figure 1d), and was modified at the 3′ end using 6-FAM amidite (Applied Biosystems) to attach a fluorescein group. To help distinguish between covalent attachment and physical adsorption, aliquots of the same fluorescently labeled DNA were added to amine-modified nanotubes that had *not* been treated with SMCC. After reacting for 48 h, both samples were washed with 2X SSPE/0.2% SDS buffer (Promega, consisting of 2 mM EDTA, 7 mM sodium dodecyl sulfate, 300 mM NaCl, and 20 mM NaH_2PO_4 with pH = 7.4) at 70 °C. Because these conditions are effective at denaturing double-stranded DNA, we also expect them to efficiently remove nonspecifically adsorbed DNA.

The use of SMCC as a covalent linker leads to obvious changes in the SWNTs. Figure 3a shows a visible-light photograph of SWNTs that were modified with SMCC and then reacted with DNA with sequence S1. The photograph shows that these SWNTs have a high affinity for water, dispersing uniformly at the bottom of a microtiter plate. In contrast, SWNTs that were amine-terminated and then exposed to DNA *without* the SMCC linker aggregate and appear to be nearly insoluble in the buffer solution. This effect can be observed clearly from optical measurements of the apparent absorbance of the solutions. Figure 3b shows the apparent absorbance at 260 nm of tubes prepared like those in Figure 3a and mechanically dispersed by shaking.[25] While the nanotubes that were not exposed to SMCC (but *were* exposed to DNA) exhibit a rapid decrease in apparent absorbance as they fall out of solution, the nanotubes that were modified with SMCC and then covalently linked to DNA show no change over the same time interval. Additional measurements (not shown) of the supernatant from tubes that were centrifuged show a higher absorption for the tubes that were covalently linked to DNA. Thus, we conclude that covalent bonding of DNA oligonucleotides to nanotubes enhances their dispersal in buffer solutions.

Measurements of the fluorescence intensity (Molecular Dynamics FluorImager 575) of the SWNTs that were modified with SMCC and then with the fluorescently labeled DNA sequence S1 yielded a median value of 4800 (in arbitrary intensity units, "I.U."), amine-modified SWNTs exposed to DNA but not modified with SMCC yielded a

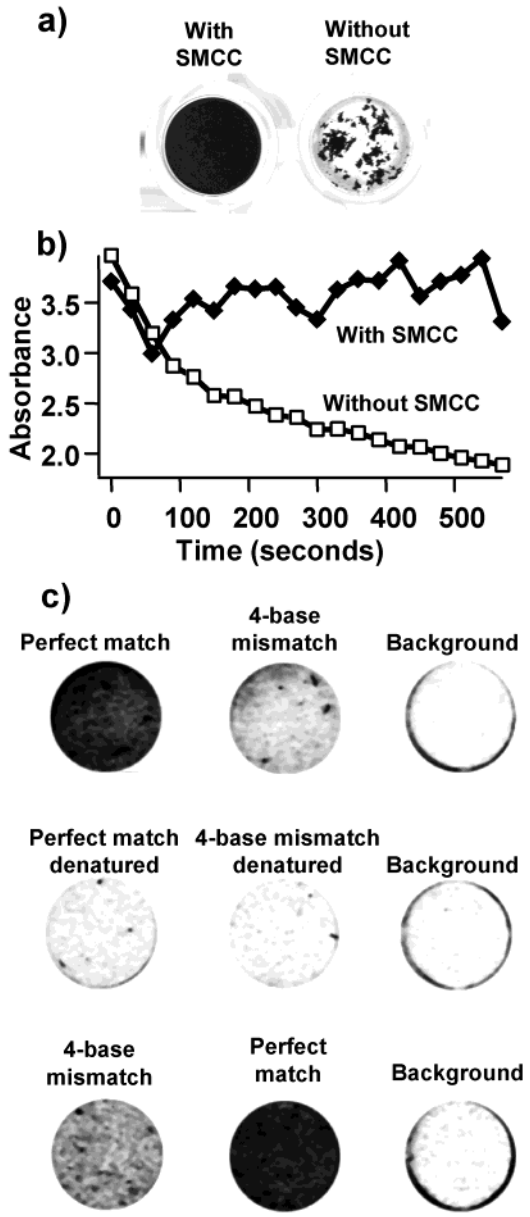

Figure 3. (a) White-light photograph showing increased dispersal upon covalent linking of DNA to single-wall nanotubes. Amine-modified nanotubes covalently linked to SMCC (left) and then linked to DNA disperse uniformly onto the bottom of the microtiter plate, while amine nanotubes exposed to DNA only, without benefit of the SMCC covalent linker (right) aggregate strongly. (b) Time-dependent optical absorption measurements (1 cm path length, 260 nm wavelength) showing that amine-modified nanotubes covalently linked to SMCC and then linked to DNA remain dispersed in solution, while amine-modified nanotubes exposed to DNA without benefit of the SMCC linker quickly aggregate and drop out of solution. (c) Fluorescence images of DNA-SWNT adducts hybridized with complementary and 4-base mismatched sequences, as described in text. The top row shows the initial hybridization. The second row shows the same samples after denaturing in urea, and the bottom row shows the same samples after hybridizing a second time with a different sequence, as described in text.

median value of 406 I.U., and an empty well yielded a value of 356 I.U. Thus, nanotubes functionalized with SMCC and then exposed to S1 under reactive conditions have higher solubility and much higher fluorescence intensity than the amine-terminated nanotubes exposed to S1 under these same conditions. This result implies that the presence of the SMCC linker significantly increases the extent of DNA functionalization and supports the presence of the covalent linkages shown in Figure 1e.

As a final test of the covalent attachment and to test the accessibility of the DNA-modified SWNTs, hybridization studies were conducted using DNA-modified SWNTs. These experiments were conducted using the oligonucleotide "S2", with the sequence (5′−HS−C_6H_{12}−T_{15}GC TTA ACG AGC AAT CG−3′) linked to the nanotubes. This oligonucleotide consists of a thiol group at the 5′ end for immobilization onto the SWNTs, a repetive sequence of thymine (T) bases, and a set of 16 additional bases for hybridization with solution-phase oligonucleotides. After immobilization onto the SWNTs, the resulting DNA−nanotube adduct was divided into two aliquots, and each was immersed in a 5 micromolar solution of DNA oligonucleotides that were labeled at the 5′ end with fluorescein. The first sequence, "S3", (5′−FAM−CG ATT GCT CGT TAA GC−3′), has 16 bases complementary to S2. The second sequence, "S4", consists of the 16-base sequence (5′−FAM−CG TTT GCA CGT TTA CC−3′) that has four-base mismatch to S2. Each sample was hybridized for 2 h at 37 °C and then shaken for 30 min. The nanotubes were washed over a 0.2 micron polycarbonate membrane with 0.2%SDS/2xSSPE buffer and placed in a 96 well microtiter plate in buffer. Figure 3 shows the resulting fluorescence image of this experiment. The top row shows the fluorescence images (black = high intensity) for hybridization of S2−SWNT with its complement, S3 (left), and with the 4-base mismatch, S4 (middle). The image at right shows the background from an empty titerplate well. Measurement of the fluorescence intensity within each well yields a median value of 1287 I.U. for the perfect match (left), 680 I.U. for the mismatch (middle), and 427 I.U. for the background. Because there is a much higher intensity from the perfectly matched pair (S2−SWNT + S3) than the mismatched pair (S2−SWNT + S4), we conclude that hybridization of the DNA−SWNT adducts with solution-phase oligonucleotides is highly specific.

To confirm that hybridization is reversible, each sample was denatured by washing with an 8.3 M urea solution. The resulting fluorescence images (Figure 3b, middle row) show only low levels of fluorescence from the two samples (intensity = 304 I.U. from perfectly matched, 267 I.U. from 4-base mismatch) comparable to the background level (intensity = 238 I.U.). Finally, the DNA-modified nanotubes were hybridized a second time. In this second hybridization, the sample that was previously hybridized with a perfect match was now hybridized with a mismatched sequence, and vice versa. The images in the bottom row of Figure 3b show that again, the fluorescence intensity of the 4-base mismatched pair S2−SWNT + S4 (bottom left, intensity = 441 I.U.) is close to that of the background (bottom right, 257 I.U.), while the relative intensity of the perfect mach S2−SWNT + S3 (bottom middle, intensity = 1073 I. U.) is much higher than either. Again, the hybridization is quite specific.

The above results strongly point to the successful synthesis of covalently linked DNA−SWNT adducts. The high stability of the adducts, combined with their accessibility in hybridization experiments, indicates that the DNA oligonucleotides are chemically bonded to the exterior of the SWNTs and are not wrapped around or intercalated within the nanotubes. Moreoever, the high accessibility to hybridization and the markedly increased affinity for aqueous buffer after linking to DNA suggests that the tubes are highly dispersed. The ability of these DNA−SWNT adducts to reversibly hybridize with high specificity to DNA molecules having complementary sequences suggests these adducts may find a number of potential uses, such as building blocks for more complex supramolecular structures and in highly selective, reversible biosensors.

Acknowledgment. The authors acknowledge helpful suggestions from Professors Eric Simanek, Robert M. Corn, Lloyd M. Smith, Richard Crooks, and Dr. Charles G. Fry. This work was sponsored by the Defense Advanced Research Projects Agency (DARPA) and the Air Force Research Laboratory, Air Force Materiel Command, USAF, under agreement number F30602-01-2-0555, and by the National Science Foundation Grant #DMR-0210806. The views and conclusions contained herein are those of the authors and should not be interpreted as necessarily representing the official policies or endorsements, either expressed or implied, of the Defense Advanced Research Projects Agency (DARPA), the Air Force Research Laboratory, or the U.S. Government.

Supporting Information Available: ^{1}H NMR spectra and ^{1}H chemical shifts of dodecylamine starting material and nanotube-dodecylamine adduct. This material is available free of charge via the Internet at http://pubs.acs.org.

References

(1) Elghanian, R.; Storhoff, J. J.; Mucic, R. C.; Letsinger, R. L.; Mirkin, C. A. *Science* **1997**, *277*, 1078.
(2) Perez, J. M.; O'Loughin, T.; Simeone, F. J.; Weissleder, R.; Josephson, L. *J. Am. Chem. Soc.* **2002**, *124*, 2856.
(3) Soto, C. M.; Srinivasan, A.; Ratna, B. R. *J. Am. Chem. Soc.* **2002**, *124*, 8508.
(4) Tsang, S. C.; Guo, Z.; Chen, Y. K.; Green, M. L. H.; Hill, H. A. O.; Hambley, T. W.; Sadler, P. J. *Angew. Chem., Int. Ed. Engl.* **1998**, *36*, 22198.
(5) Guo, Z.; Sadler, P. J.; Tsang, S. C. *Adv. Mater.* **1998**, *10*, 701.
(6) Chen, R. J.; Zhang, Y.; Wang, D.; Dai, H. *J. Am. Chem. Soc.* **2001**, *123*, 3838.
(7) Shim, M.; Kam, N. W. S.; Chen, R. J.; Li., Y.; Dai, H. *Nano Lett.* **2002**, *2*, 285.
(8) Dillon, A. C.; Gennett, T.; Jones, K. M.; Alleman, J. L.; Parilla, P. A.; Hebert, M. J. *Adv. Mater.* **1999**, *11*, 1354.
(9) Rinzler, A. G.; Liu, J.; Dai, H.; Nikolaev, P.; Huffman, C. B.; Rodriguez-Macias, F. J.; Boul, P. J.; Lu, A. H.; Heymann, D.; Colbert, D. T.; Lee, R. S.; Fischer, J. E.; Rao, A. M.; Eklund, P. C.; Smalley, R. E. *Appl. Phys. A* **1998**, *67*, 29.
(10) Holzinger, M.; Vostrowsky, O.; Hirsch, A.; Hennrich, F.; Kappes, M.; Weiss, R.; Jellen, F. *Angew. Chem., Int. Ed. Engl.* **2001**, *40*, 4002.
(11) Strother, T.; Cai, W.; Zhao, X.; Hamers, R. J.; Smith, L. M. *J. Am. Chem. Soc.* **2000**, *122*, 1205−1209.
(12) Barth, G.; Linder, R.; Bryson, C. *Surf. Interface Anal.* **1988**, *11*, 307.
(13) Wagner, C. D.; Naumkin, A. V.; Kraut-Vass, A.; Allison, J. W.; Powell, C. J.; Rumble, J. R., Jr. NIST X-ray Photoelectron Spectroscopy Database, NIST Standard Reference Database 20, Version 3.2; 3.2 ed.; National Institute of Standards and Technology, 2002; Vol. 2002.
(14) Goldoni, A.; Larciprete, R.; Gregoratti, L.; Kaulich, B.; Kiskinova, M.; Zhang, Y.; Dai, H.; Sangaletti, L.; Parmigiani, F. *Appl. Phys. Lett.* **2002**, *80*, 2165.
(15) Mawhinney, D. B.; Naumenko, V.; Kuznetsova, A.; Yates, J. T., Jr.; Liu, J.; Smalley, R. E. *Chem. Phys. Lett.* **2000**, *324*, 213.
(16) Hu, H.; Bhowmik, P.; Zhao, B.; Hamon, M. A.; Itkis, M. E.; Haddon, R. C. *Chem. Phys. Lett.* **2001**, *345*, 25.
(17) Chen, J.; Hammon, M. A.; Hu, H.; Chen, Y.; Rao, A. M.; Eklund, P. C.; Haddon, R. C. *Science* **1998**, *282*, 95.
(18) Ascah, T. L.; Kallury, K. M. R.; Szafranski, C. A.; Corman, S. D.; Liu, F. *J. Liq. Chromatogr., Relat. Technol.* **1996**, *19*, 3049.
(19) Lin, Z.; Strother, T.; Cai, W.; Cao, X.; Smith, L. M.; Hamers, R. J. *Langmuir* **2002**, *18*, 788.
(20) Moulder, J. F.; Stickle, W. F.; Sobol, P. E.; Bomben, K. D. *Handbook of X-ray Photoelectron Spectroscopy*; Perkin-Elmer Corporation: Eden Prairie, 1992.
(21) Pretsch, E.; Simon, W.; Seibl, J.; Clerc, T. *Tables of Spectral Data for Structure Determination of Organic Compounds*, 2nd ed.; Springer-Verlag: Berlin, 1989.
(22) Banerjee, S.; Wong, S. S. *J. Am. Chem. Soc.* **2002**, *124*, 8940.
(23) Yang, W.; Butler, J. E.; Cai, W.; Carlisle, J.; Gruen, D.; Knickerbocker, T.; Russell, J. N., Jr.; Smith, L. M.; Hamers, R. J. *Nature-Materials* **2002**, submitted.
(24) Knickerbocker, T.; Strother, T.; Schwartz, M. P.; Russell, J. N., Jr.; Butler, J. E.; Hamers, R. J. *Langmuir* **2002**, submitted.
(25) We use the term "apparent absorbance" because this measurement cannot distinguish between scattering and actual absorbance. Measurements were obtained over the entire 240−800 nm spectral range; no significant differences were observed at different wavelengths.

NL025729F